·论 著·

叉头框蛋白A1基因敲除对苯并[a]芘恶性转化细胞THBEc1转录组的影响

马 雪[1], 李璐迪[1], 王 裕[2], 邢云昆[1], 付娟玲[1], 姚碧云[1], 赵 鹏[1]
(1. 北京大学公共卫生学院毒理学系, 食品安全毒理学研究与评价北京市重点实验室, 北京 100191;
2. 中国疾病预防控制中心环境与健康相关产品安全所, 北京 100021)

摘要: 目的 研究叉头框蛋白A1(*FOXA1*)基因敲除对苯并[a]芘(BaP)恶性转化细胞THBEc1转录组的影响,探讨*FOXA1*在BaP致癌作用中的可能机制。**方法** 以*FOXA1*敲除细胞THBEc1-Δ*FOXA1*-c34和对照细胞THBEc1-ctrl为研究模型,采用Western印迹法测定FOXA1蛋白表达水平,分别采用克隆形成实验和Transwell实验测定细胞增殖和迁移能力。采用二代测序技术检测THBEc1-Δ*FOXA1*-c34与THBEc1-ctrl细胞间差异表达基因,并通过实时荧光定量PCR(RT-qPCR)对转录组测序结果进行验证。采用DAVID数据库对差异表达基因进行基因本体论(GO)和京都基因与基因百科全书(KEGG)通路富集分析。采用STRING 11.5数据库和Cytoscape 3.8.2对差异基因编码蛋白进行网络分析。**结果** THBEc1-Δ*FOXA1*-c34细胞未检出FOXA1表达,且增殖和迁移能力均低于THBEc1-ctrl(P<0.01)。转录组差异分析共检出1332个基因在THBEc1-Δ*FOXA1*-c34与THBEc1-ctrl细胞间的表达差异倍数>2或<0.5(错误发现率<0.05),其中691个基因在THBEc1-Δ*FOXA1*-c34中表达高于THBEc1-ctrl,641个基因在THBEc1-Δ*FOXA1*-c34中表达低于THBEc1-ctrl。RT-qPCR验证的47个基因的表达差异和统计学P值与转录组测序结果一致。差异表达基因涉及多种生物学过程,主要包括血管生成、细胞增殖、迁移、黏附、炎症反应、免疫应答、信号转导[包括肿瘤坏死因子(TNF)、丝裂原活化蛋白激酶(MAPK)、磷脂酰肌醇-3-激酶/蛋白激酶B和转化生长因子β(TGF-β)等通路]和代谢等。在349个差异表达基因所编码的蛋白质形成的相互作用网络中,共发现分别以C-C趋化因子配体3(CCL3)、O-聚糖合酶葡糖胺基(N-乙酰基)转移酶3(GCNT3)、基质金属蛋白酶3(MMP3)和卷曲蛋白8(FZD8)为种子节点的4个核心功能模块。核心功能模块主要参与免疫应答和炎症反应、O-聚糖加工、胶原分解代谢过程以及典型WNT通路等。**结论** 敲除*FOXA1*后BaP恶性转化细胞THBEc1转录组明显改变,增殖和迁移能力明显降低。*FOXA1*敲除可能通过直接或间接影响TNF,MAPK和WNT等通路抑制细胞增殖和迁移。FOXA1可能作为BaP致癌的潜在生物标志物和肺癌的潜在治疗靶点。

关键词: 苯并[a]芘; 叉头框蛋白A1; THBEc1细胞
中图分类号: R99 **文献标志码:** A **文章编号:** 1000-3002-(2022)03-0185-12
DOI: 10.3867/j.issn.1000-3002.2022.03.004

苯并[a]芘(benzo[a]pyrene,BaP)属于多环芳烃类化合物,可经Ⅰ相和Ⅱ相代谢酶代谢活化后发挥毒作用,与癌症如肺癌、膀胱癌、食管癌和皮肤癌等发生有关[1]。实验研究也证实,BaP可诱发实验动物肿瘤以及体外培养细胞的恶性转化[2-3]。因暴露因素明确,体外细胞恶性转化已成为研究化学致癌机制的重要方法。国内外学者利用BaP终致癌物(+)-反式-7,8-二氢二醇-9,10-环氧BaP(anti-benzo[a]pyrene-7,8-diol-9,10-epoxide,anti-BPDE)成功诱导人支气管上皮细胞16HBE和BEAS-2B恶性转化,并以此为模型开展了大量工作,在研究BaP致癌机制,特别是表观遗传机制方面取得了重要进展。研究发现,微RNA(microRNA,miRNA)miR-106a,miR-506和miR-377-3p等,长链非编码RNA AF118081,LOC728228和DQ786227等,以及环状RNA Circ_CARM1等分别在anti-BPDE诱导16HBE和BEAS-2B细胞恶性转化过程中发挥重要作用[4-10]。尽管对BaP致癌机制已开展了大量研究

基金项目: 国家自然科学基金(81370079); 国家自然科学基金(81001253); 北京市自然科学基金(7132122)
作者简介: 马 雪,硕士研究生,主要从事细胞与分子毒理学研究。
通讯作者: 赵 鹏, E-mail: zhaopeng@bjmu.edu.cn

工作，并发现了若干BaP致癌的遗传和表观遗传事件，但综合现有研究证据，尚不能完全阐明BaP通过影响哪些信号通路和网络使正常细胞恶性转化为肿瘤细胞，相关机制仍需进一步研究。叉头框蛋白A1（forkhead-box A1，FOXA1）又称肝细胞核因子3α（hepatocyte nuclear factor-3α，HNF-3α），是具有开放染色质能力的先锋转录因子[11]。在表观遗传和其他辅因子的作用下，FOXA1可影响与发育和代谢等有关的基因的表达，从而参与肝、消化道上皮、肺上皮、胰腺、肠和神经元等内胚层衍生器官的发育以及机体的新陈代谢[12-13]。有研究发现，FOXA1参与肿瘤细胞增殖、侵袭、迁移和凋亡等的调控，在肺癌、膀胱癌、乳腺癌和前列腺癌等多种肿瘤中表达失调，且与肿瘤的发生和发展和预后密切相关[14-19]。本课题组利用BaP诱导16HBE细胞恶性转化，建立了T-16HBE-c1（THBEc1）细胞系。THBEc1细胞形态虽无明显改变，但可复层生长和锚定非依赖性生长，在裸鼠体内可成瘤，并呈高迁移和侵袭表型[3]。通过构建*FOXA1*敲除THBEc1细胞模型THBEc1-Δ*FOXA1*-c34开展的研究发现，敲除*FOXA1*能抑制THBEc1细胞的体外克隆形成和细胞迁移能力及裸鼠体内成瘤和转移能力，提示*FOXA1*可能在BaP致癌中发挥癌基因作用[17]。本研究以THBEc1-Δ*FOXA1*-c34和对照细胞THBEc1-ctrl为模型，利用二代测序技术筛选模型细胞间差异表达基因，并对差异基因进行生物信息学分析，识别FOXA1可能参与调控的生物学过程、信号通路和网络，为探讨FOXA1在BaP致癌作用中的可能机制提供线索。

1 材料与方法

1.1 主要试剂和仪器

胰蛋白酶、青霉素、链霉素，美国Sigma公司，TRIzol®试剂，美国Invitrogen公司；FastKing cDNA第一链合成试剂盒、SuperReal PreMix Plus（SYBR Green）和Pro-Light HRP化学发光检测试剂盒，北京天根生化科技有限公司；兔抗人FOXA1单克隆抗体，英国Abcam公司；小鼠抗人β肌动蛋白单克隆抗体和辣根过氧化物酶标记的山羊抗兔IgG和山羊抗小鼠IgG抗体均购自北京中杉金桥生物技术有限公司。SCI-I65D CO_2恒温培养箱，日本ASTEC公司；MEM培养基和胎牛血清，美国Gibco公司。

1.2 细胞培养

BaP恶性转化细胞THBEc1由本课题组构建并保存。*FOXA1*基因敲除THBEc1单克隆细胞THBEc1-Δ*FOXA1*-c34为利用CRISPR/Cas9技术经*FOXA1*双切口酶质粒转染和筛选所获的THBEc1细胞单克隆株，由本实验室构建并保存[17]。对照细胞THBEc1-ctrl由本实验室构建并保存，其*FOXA1*外显子序列及FOXA1蛋白表达水平与THBEc1细胞均无差异[17]。细胞培养均使用含10%胎牛血清的MEM培养液（完全培养液），培养于37℃，5% CO_2饱和湿度培养箱中。

1.3 Western印迹法检测FOXA1蛋白表达

收集对数生长期细胞，使用RIPA裂解液提取细胞总蛋白，Bradford法测定蛋白浓度。将30 μg蛋白样品经12% SDS-PAGE分离，再经湿式电转法转印至硝酸纤维素膜（NC膜）。NC膜经5%脱脂奶粉室温封闭2 h后，分别与兔抗人FOXA1抗体（1∶3000）和小鼠抗人β肌动蛋白抗体（1∶3000）4℃孵育过夜，继而与二抗（1∶20 000）室温孵育2 h。经TBST清洗后，使用Pro-Light HRP化学发光检测试剂盒检测蛋白条带，利用天能化学发光成像分析系统获取图像。利用Image J软件分析每个条带积分吸光度值，以目的蛋白与内参蛋白的积分吸光度比值表示目的蛋白表达水平。

1.4 克隆形成实验计数克隆数目和克隆形成率

将对数生长期细胞以每皿200个接种于6 cm直径培养皿，每组细胞设5个平行皿。培养14 d后，使用磷酸盐缓冲液清洗细胞2次，甲醇室温固定15 min。固定结束，使用0.01%结晶紫染液染色15 min。高纯水清洗后，晾干拍照。计数克隆数目并计算克隆形成率，克隆形成率（%）=克隆数/接种细胞数×100%。

1.5 迁移实验计数迁移细胞数

将对数生长期细胞经无血清MEM培养液饥饿24 h后，重悬于无血清MEM培养液中并调整细胞密度为6.67×10^8 L^{-1}。将该细胞悬液150 μL（1×10^5个细胞）接种于8 μm孔径Transwell小室（Thermo）的上室，下室加入500 μL含10%胎牛血清的MEM完全培养液。培养48 h后，用棉签擦去上室中的非迁移细胞。上室下表面的迁移细胞经甲醇固定后，用苏木素染色。每次实验均在显微镜下计数每种细胞10个不同视野（20×）的迁移细胞数，以每视野平均细胞数表示细胞的迁移能力。实验重复3次。

1.6 转录组测序样品收集

将THBEc1-Δ*FOXA1*-c34和THBEc1-ctrl细胞分别以每皿6.0×10^5个接种于6 cm直径培养皿。接种后48 h，细胞处于对数生长期时，弃培养液，每皿加

入2.5 mL TRIzol®试剂。室温静置5 min，轻轻吹打使细胞完全裂解后收集于冻存管中，−80℃保存。

1.7 转录EBseq算法筛选差异表达基因

细胞总RNA提取与转录组测序委托上海卓灏医药科技有限公司完成。根据定量数据counts值，利用EBseq算法筛选差异表达基因，以差异倍数（fold change，FC）>2或<0.5且错误发现率（false discovery rate，FDR）<0.05为筛选条件。

1.8 实时荧光定量PCR（real-time quantitative PCR，RT-qPCR）测定mRNA水平

利用TRIzol®试剂提取对数生长期细胞总RNA。以总RNA为模板，使用FastKing cDNA第一链合成试剂盒合成cDNA。通过RT-qPCR检测差异表达基因的mRNA水平，以*GAPDH*作为内参，计算相对表达量，并与转录组测序结果进行比较。引物序列见表1。

Tab.1 Primer sequences of real-time quantitative PCR（RT-qPCR）

Gene	Primer sequence (5′−3′)	
	Forward	Reverse
AKT3	TGAAGTGGCACACACTCTAACT	CCGCTCTCTCGACAAATGGA
ALDH3A1	CTCCAGCAACGACAAGGTGA	GGCAGAGAGTGCAAGGTGAT
ALDH3B2	ATGAAGGATGAACCACGGTCC	GTTCCAGGGTGCGATGATGA
AOC1	CAGTGACCAAGTACCGGGAG	AGGCCACCAGGTCCTCATTT
ARPC2	GCAGATTTCGATGGGGTCCTC	ACTCCCGTACACCCTCTTTAAT
BMPR2	GGCAGCAGTATACAGATAGGTGA	ACTGCCCTGTTACTGCCATT
CACNG4	GTGTGCTGCATCGAAGGGAT	GGACGATGTTGTTCTTGCGG
CCL22	AAGCTGAGGTCAGTCTCCCA	CAGCAACATCCCAGGCAAAG
CDK6	ACAGAGCACCCGAAGTCTTG	GGGAGTCCAATCACGTCCAA
CMTM7	GGTAGCCGGAGCGATCTTTG	CTGCATCTGTGGACTGGGTT
CPS1	CAGCAATCATTCCGGCCAAG	TTCCGTGGCAAACAGCTTGA
CREB5	CCCTGCCCAACCCTACAATG	GGACCTTGCATCCCCATGAT
CYP1B1	AAGTTCTTGAGGCACTGCGAA	GGCCGGTACGTTCTCCAAAT
DLC1	ATGATCGCCGAGTGCAAGAA	CGAGTGCTTCCAGAGTGAGG
DUSP4	GGCATCACGGCTCTGTTGAAT	GTCGGCCTTGTGGTTATCTTC
DUSP5	TGTCGTCCTCACCTCGCTA	GGGCTCTCTCACTCTCAATCTTC
FGFR2	CCTCTCTTCAACGGCAGACA	TGCCCAGTGTCAGCTTATCT
FOLR1	AAGAGCGGGTACTGAACGTG	CGCACTTGTTAAACCCTGAAGT
FZD10	GCTCAAGTGCTCCCCGATTA	GCCTCCATGCACAGGTAGTT
GATA3	GCCCCTCATTAAGCCCAAG	TTGTGGTGGTCTGACAGTTCG
GDF6	CCTATCACTGCGAGGGTGTAT	GATGGGAGTCAATTTGGTGGG
GLUL	GGTGTACATGTCCCTGCCTC	TCCACTCAGGCAACTCTTCC
GOLGA7B	GTTGGCGGGAGGTGTTAGAA	TCTCTGGTCTCTGGGTAGGC
GSN	CGTCATGCTTCTGGACACCT	CTCGATGTACCGCTTAGCAGA
HSPB1	CTACATCTCCCGGTGCTTCA	TTTACTTGGCGGCAGTCTCAT
IDH1	GTTTAGGCCGCAGGAGAGTT	AGGCCAGCAGAAGTCCAAAA
IGF1R	TCGACATCCGCAACGACTATC	CCAGGGCGTAGTTGTAGAAGAG
IKZF2	GCCTGTAGAAGAAGGGACGC	CCTTGTGCTCCTCCAGTGAA
ITPR1	GCGGAGGGATCGACAAATGG	TGGGACATAGCTTAAAGAGGCA
KSR1	GGGGAAGGAAGTCAGTGAGA	TCTCCAGCATGTCCATCAGC
MAOA	GGGTCCTTCCCACCCTTTG	ATCTCTTCTCTTGGCCTGAAATG
MAP2K6	GCATTTCCATCTTGATTCCCTG	TTTCGCTTCTTGCCTTTCGAC
MAPK10	TATGTGGAGAATCGGCCCAAG	GCTTTGAGTTTATTGTGCTCGG

Tab.1 continued

Gene	Primer sequence (5'-3')	
	Forward	Reverse
PIKFYVE	CATATTGCCACAAGGGCACA	ACTGAGTCACTGTCGGGAGA
PKN3	GGCAGGAACGCATCTTCTCTA	CCTCTCGCAGTGTTGTTGG
PLCE1	GCTTCTTAACACGGGACTTGG	CTTCAAGGGCATTGTGCTCTC
PLOD2	ACTGAAGGTCTTTGCAGGCT	AATTTGCAACCACCTCCCTGA
PRKCA	TTTTCCCGGGCAACGACTC	TTTCCCAAACCCCCAGATGA
PTHLH	GCCGCCGCCTCAAAAGA	GGCTTGGAGTTAGGGGACAC
RNF128	AAGCTTTGGGAATTGAGGTGGA	TTGTTGACTGCACGTGTTCC
RORA	ACCCAGACATTGTGCGACTT	CCTGACCCCGATCACCAAAA
RUNX2	CCCTGAACTCTGCACCAAGT	GGGGTGGTAGAGTGGATGGA
SNAI2	CGAACTGGACACACATACAGTGAT	GAGAGGCCATTGGGTAGCTG
TCF7L1	TCGTCCCTGGTCAACGAGT	ACTTCGGCGAAATAGTCCCG
TGFB2	CCATCCCGCCCACTTTCTAC	AGCTCAATCCGTTGTTCAGGC
TMEM98	TCGGTCAGAATGTGTGGCAA	AAACCCAAACCTGCAAGGGA
TRAF5	CCACTCGGTGCTTCACAAC	GTACCGGCCCAGAATAACCT
GAPDH	GGAGCGAGATCCCTCCAAAAT	GGCTGTTGTCATACTTCTCATGG

AKT3: AKT serine/threonine kinase 3; *ALDH3A1*: aldehyde dehydrogenase 3 family member A1; *ALDH3B2*: aldehyde dehydrogenase 3 family member B2; *AOC1*: amine oxidase copper containing 1; *ARPC2*: actin related protein 2/3 complex subunit 2; *BMPR2*: bone morphogenetic protein receptor type 2; *CACNG4*: calcium voltage-gated channel auxiliary subunit gamma 4; *CCL22*: C-C motif chemokine ligand 22; *CDK6*: cyclin dependent kinase 6; *CMTM7*: CKLF like MARVEL transmembrane domain containing 7; *CPS1*: carbamoyl-phosphate synthase 1; *CREB5*: cAMP responsive element binding protein 5; *CYP1B1*: cytochrome P450 family 1 subfamily B member 1; *DLC1*: deleted in liver cancer 1; *DUSP4*: dual specificity phosphatase 4; *DUSP5*: dual specificity phosphatase 5; *FGFR2*: fibroblast growth factor receptor 2; *FOLR1*: folate receptor alpha; *FZD10*: frizzled class receptor 10; *GATA3*: GATA binding protein 3; *GDF6*: growth differentiation factor 6; *GLUL*: glutamate-ammonia ligase; *GOLGA7B*: golgin A7 family member B; *GSN*: gelsolin; *HSPB1*: heat shock protein family B (small) member 1; *IDH1*: isocitrate dehydrogenase (NADP(+)) 1; *IGF1R*: insulin like growth factor 1 receptor; *IKZF2*: IKAROS family zinc finger 2; *ITPR1*: inositol 1,4,5-trisphosphate receptor type 1; *KSR1*: kinase suppressor of ras 1; *MAOA*: monoamine oxidase A; *MAP2K6*: mitogen-activated protein kinase kinase 6; *MAPK10*: mitogen-activated protein kinase 10; *PIKFYVE*: phosphoinositide kinase, FYVE-type zinc finger containing; *PKN3*: protein kinase N3; *PLCE1*: phospholipase C epsilon 1; *PLOD2*: procollagen-lysine,2-oxoglutarate 5-dioxygenase 2; *PRKCA*: protein kinase C alpha; *PTHLH*: parathyroid hormone-like hormone; *RNF128*: ring finger protein 128; *RORA*: RAR related orphan receptor A; *RUNX2*: RUNX family transcription factor 2; *SNAI2*: snail family transcriptional repressor 2; *TCF7L1*: transcription factor 7 like 1; *TGFB2*: transforming growth factor beta 2; *TMEM98*: transmembrane protein 98; *TRAF5*: TNF receptor associated factor 5; *GAPDH*: glyceraldehyde-3-phosphate dehydrogenase.

1.9 生物信息学分析

利用DAVID数据库对差异表达基因进行基因本体论(gene ontology,GO)和京都基因与基因百科全书(kyoto encyclopedia of genes and genomes,KEGG)通路富集分析。利用STRING 11.5数据库对差异表达基因编码蛋白进行蛋白-蛋白相互作用(protein-protein interaction,PPI)网络分析,下载PPI标签分隔符文件。将数据按combined score>0.8进行筛选,将筛选后的PPI数据导入Cytoscape 3.8.2软件,构建可视化PPI网络图。利用cytoHubba插件计算Degree值,设定网络中图形颜色和大小分别反映Log_2(FC)和Degree值。利用MCODE插件,以Degree cutoff值为2,K-Core为2,对PPI网络进行聚类分析,筛选得分>6的核心功能模块。

1.10 统计学分析

利用SPSS 26.0软件对实验数据进行统计学分析,Graphpad Prism 8.0软件进行图表绘制。数据均为3次重复实验结果,以$\bar{x}\pm s$表示。两组间比较采用t检验,$P<0.05$表示差异具有统计学意义。

2 结果

2.1 THBEc1-Δ*FOXA1*-c34中FOXA1蛋白表达水平

在利用课题组前期CRISPR/Cas9技术制备的THBEc1-Δ*FOXA1*-c34中未检出FOXA1蛋白表达(图1),表明细胞模型可靠。

2.2 *FOXA1*敲除对THBEc1细胞增殖和迁移的影响

经过多次($n>20$)传代培养的THBEc1-Δ*FOXA1*-c34细胞克隆形成率和每视野迁移细胞数均明显低于THBEc1-ctrl细胞对照组($P<0.01$)(图2),表明敲除*FOXA1*基因可抑制细胞增殖和体外迁移能力。

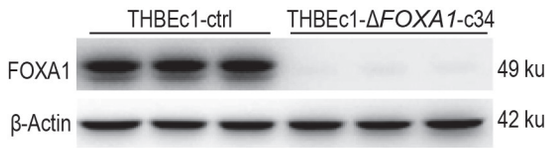

Fig.1 Protein expression levels of forkhead box protein A1 (FOXA1) in THBEc1-Δ*FOXA1*-c34 and THBEc1-ctrl cells by Western blotting. THBEc1: transformed human bronchial epithelial 16HBE cells; THBEc1-ctrl: control cells; THBEc1-Δ*FOXA1*-c34: *FOXA1* knockout THBEc1 cells.

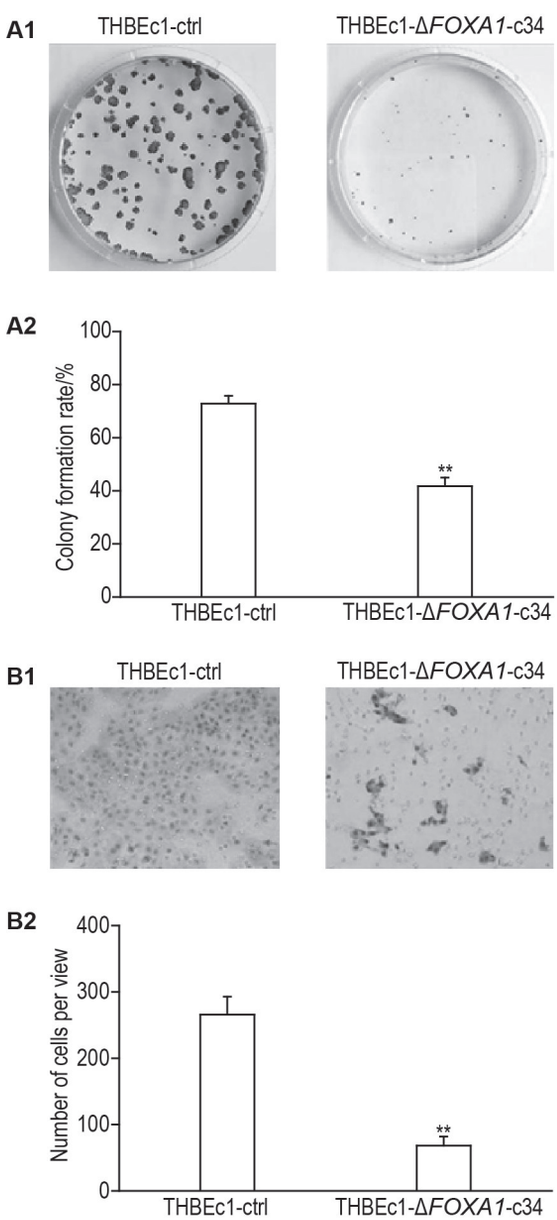

Fig.2 Effect of *FOXA1* knockout on cell proliferation (A) and migration (B) *in vitro*. A1: photos of clone formation experiment; A2: clone formation rate (n=5); B1: pohotos of migration experiment; B2: counting results of migration experiment. Colony formation rate (%) = number of clones/number of cells seeded ×100%. $\bar{x}\pm s$, n=3. $^{**}P$<0.01, compared with THBEc1-ctrl cells.

2.3 THBEc1-Δ*FOXA1*-c34 和 THBEc1-ctrl 细胞转录组差异分析

在THBEc1-Δ*FOXA1*-c34和THBEc1-ctrl细胞中分别共检出19150±327和19540±467个基因，所检出全部基因的表达FC（与THBEc1-ctrl细胞比较）和FDR值如图3所示。在THBEc1-Δ*FOXA1*-c34和THBEc1-ctrl细胞中共筛选出1332个基因的表达FC>2或<0.5，且FDR<0.05，其中691个基因在THBEc1-Δ*FOXA1*-c34细胞中的表达高于THBEc1-ctrl细胞，641个基因在THBEc1-Δ*FOXA1*-c34细胞中表达低于THBEc1-ctrl细胞。

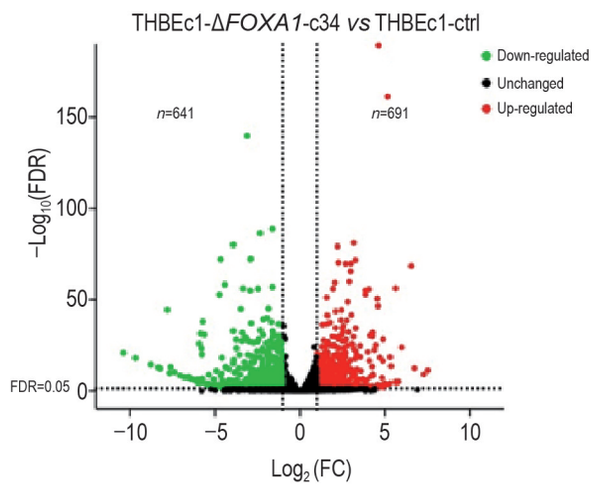

Fig.3 Fold change (FC) and false discovery rate (FDR) value of genes between THBEc1-Δ*FOXA1*-c34 and THBEc1-ctrl cells. Compared with THBEc1-ctrl cells, 641 genes (green) were down-regulated, and 691 genes (red) were up-regulated in THBEc1-Δ*FOXA1*-c34 cells.

2.4 THBEc1-Δ*FOXA1*-c34 和 THBEc1-ctrl 细胞差异表达基因的验证

为验证转录组测序结果，本研究利用RT-qPCR对随机选择的47个差异表达基因在模型细胞中的mRNA表达水平进行了检测，结果如图4所示。与THBEc1-ctrl细胞比较，维甲酸相关孤核受体A（RAR related orphan receptor A, *RORA*），C-C趋化因子配体22（C-C motif chemokine ligand 22, *CCL22*）、双特异性磷酸酶5（dual specificity phosphatase 5, *DUSP5*）、双特异型磷酸酶4（dual specificity phosphatase 4, *DUSP4*）、丝氨酸/苏氨酸蛋白激酶3（AKT serine/threonine kinase 3, *AKT3*）、趋化素样因子超家族成员7（CKLF like MARVEL transmembrane domain containing 7, *CMTM7*）、肝癌缺失基因-1（deleted in liver cancer 1, *DLC1*）、golgin A7家族成员B（golgin A7 family

member B, *GOLGA7B*)等8个基因在THBEc1-Δ*FOXA1*-c34细胞中上调;钙电压门控通道辅助亚基γ4(calcium voltage-gated channel auxiliary subunit gamma 4, *CACNG4*)、乙醛脱氢酶3A1(aldehyde dehydrogenase 3 family member A1, *ALDH3A1*)、跨膜蛋白98(transmembrane protein 98, *TMEM98*)、磷脂酶Cε1(phospholipase C epsilon 1, *PLCE1*)、生长分化因子6(growth differentiation factor 6, *GDF6*)、cAMP反应元件结合蛋白5(cAMP responsive element binding protein 5, *CREB5*)、细胞色素P4501B 1(cytochrome P450 family 1 subfamily B member 1, *CYP1B1*)、IKAROS家族锌指2(IKAROS family zinc finger 2, *IKZF2*)、乙醛脱氢酶3B2(aldehyde dehydrogenase 3 family member B2, *ALDH3B2*)、Ras激酶抑制因子(kinase suppressor of ras 1, *KSR1*)、含铜氨氧化酶1(amine oxidase copper containing 1, *AOC1*)、单胺氧化酶A(monoamine oxidase A, *MAOA*)、异柠檬酸脱氢酶1〔isocitrate dehydrogenase (NADP(+)) 1, *IDH1*〕、丝裂原活化蛋白激酶激酶6(mitogen-activated protein kinase kinase 6, *MAP2K6*)、热休克蛋白B1〔heat shock protein family B(small) member 1, *HSPB1*〕、转录因子7样1(transcription factor 7 like 1, *TCF7L1*)、肿瘤坏死因子受体相关因子5(TNF receptor associated factor 5, *TRAF5*)、环指蛋白128(ring finger protein 128, *RNF128*)、转化生长因子β2(transforming growth factor-β2, *TGFB2*)、骨形态发生蛋白2型受体(bone morphogenetic protein receptor type 2, *BMPR2*)、Ⅲ型磷脂酰肌醇3-磷酸5-激酶(phosphoinositide kinase, *PIKFYVE*)、蜗牛家族转录抑制因子2(snail family transcriptional repressor 2, *SNAI2*)、凝溶胶蛋白(gelsolin, *GSN*)、氨基甲酰磷酸合成酶1(carbamoyl-phosphate synthase 1, *CPS1*)、丝裂原活化蛋白激酶10(mitogen-activated protein kinase 10, *MAPK10*)、卷曲蛋白10(frizzled class receptor 10, *FZD10*)、蛋白激酶Cα(protein kinase C alpha, *PRKCA*)、GATA结合蛋白3(GATA binding protein 3, *GATA3*)、赖氨酸羟化酶2(procollagen-lysine, 2-oxoglutarate 5-dioxygenase 2, *PLOD2*)、谷氨酸氨连接酶(glutamate-ammonia ligase, *GLUL*)、胰岛素样生长因子1受体(insulin like growth factor 1 receptor, *IGF1R*)、成纤维细胞生长因子受体2(fibroblast growth factor receptor 2,

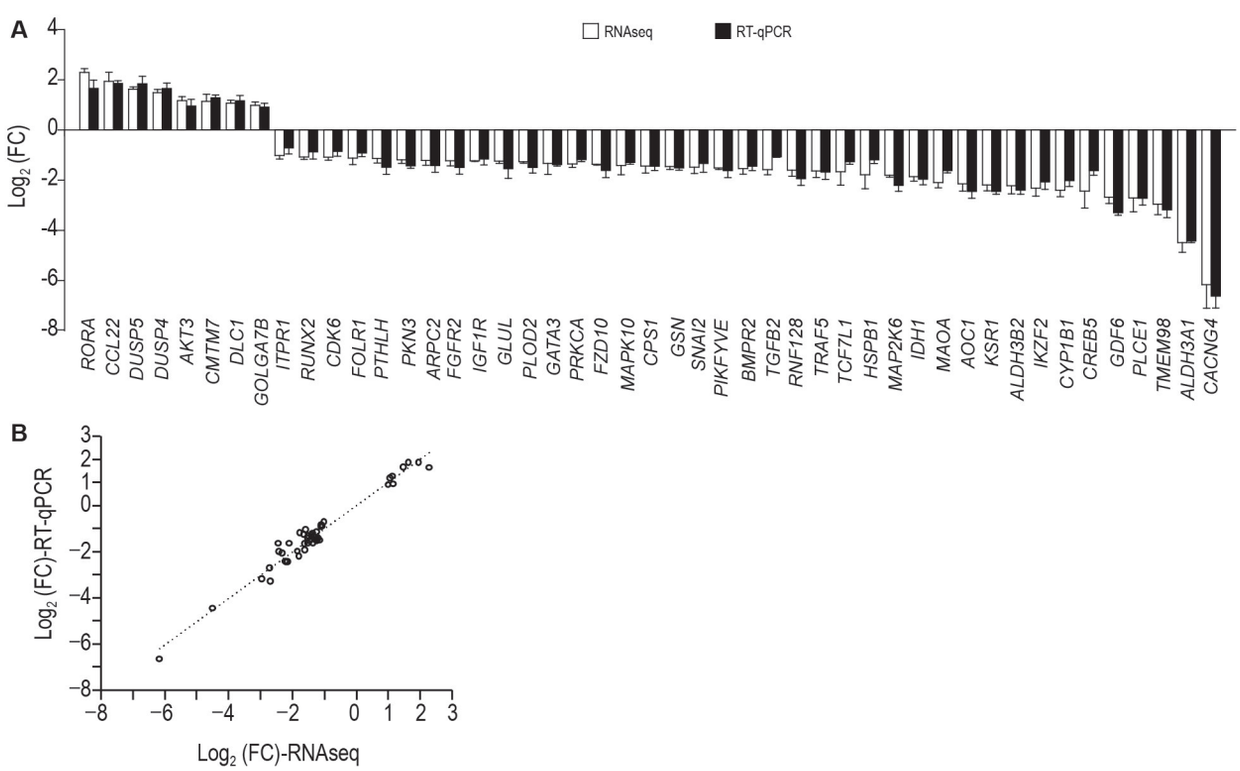

Fig.4 Comparison of transcriptome sequencing (RNAseq) and RT-qPCR results of THBEc1-Δ*FOXA1*-c34 cells. A: logarithm of gene expression FC detected by RNAseq and RT-qPCR, respectively. FC refers to the ratio of THBEc1-Δ*FOXA1*-c34 to THBEc1-ctrl cells. Compared with the THBEc1-ctrl cells, FDR (by RNAseq) and *P* value (by RT-qPCR) of the indicated genes is less than 0.05. B: linear correlation between the logarithm of gene expression FC detected by the two methods.

FGFR2)、肌动蛋白相关蛋白复合体2(actin related protein 2/3 complex subunit 2, *ARPC2*)、蛋白激酶C相关激酶N3(protein kinase N3, *PKN3*)、甲状旁腺激素样激素(parathyroid hormone-like hormone, *PTHLH*)、叶酸受体1基因(folate receptor alpha, *FOLR1*)、细胞周期蛋白依赖性激酶6(folate receptor alpha, *CDK6*)、RUNX家族转录因子2(RUNX family transcription factor 2, *RUNX2*)和肌醇1,4,5-三磷酸受体1型(inositol 1,4,5-trisphosphate receptor type 1, *ITPR1*)等39个基因在THBEc1-Δ*FOXA1*-c34中下调,且差异均有统计学意义($P<0.05$)。转录组测序与RT-qPCR所检出的上述基因表达差异倍数一致,相关系数$R=0.9808$,表明转录组测序结果可靠。

2.5 THBEc1-Δ*FOXA1*-c34和THBEc1-ctrl细胞差异表达基因的生物信息学分析

GO分析(图5)发现,差异表达基因涉及生物过程203项、分子功能44项、细胞组分30项。富集的生物过程包括血管生成、细胞黏附、基因表达的正调控、丝裂原活化蛋白激酶(mitogen-activated protein kinases, MAPK)活性的激活、肽基酪氨酸磷酸化的正调控、细胞增殖的负调控、炎症反应、内肽酶活性的负调控、表皮发育和细胞生长调节等。富集的分子功能涉及生长因子活性、细胞外基质结构组成、细胞因子活性、肝素结合、金属内肽酶活性、丝氨酸型内肽酶抑制剂活性、RNA聚合酶Ⅱ核心启动子近端区域序列特异性DNA结合、Ras鸟苷酸交换因子活性和胰岛素样生长因子Ⅰ结合和整合素结合等。富集的细胞组分有细胞外间隙、胞外域、蛋白质细胞外基质、质膜的组成部分、高尔基体腔、质膜、细胞外基质、胞外外泌体、细胞表面和黏着斑等。

KEGG通路分析(图6)发现,差异表达基因富集于36条信号通路,主要涉及到细胞因子和细胞因子受体相互作用、补体和凝血级联通路、肿瘤坏死因子(tumor necrosis factor, TNF)通路、癌症的转录失调、癌症中的蛋白多糖通路、瞬时受体电位(transient receptor potential, TRP)通道的炎症介质调节、调控干细胞多能性的信号通路、Hippo通路、Rap1通路、癌症通路、造血细胞谱系、磷脂酰肌醇-3-激酶/蛋白激酶B(phosphatidylinositol-4,5-

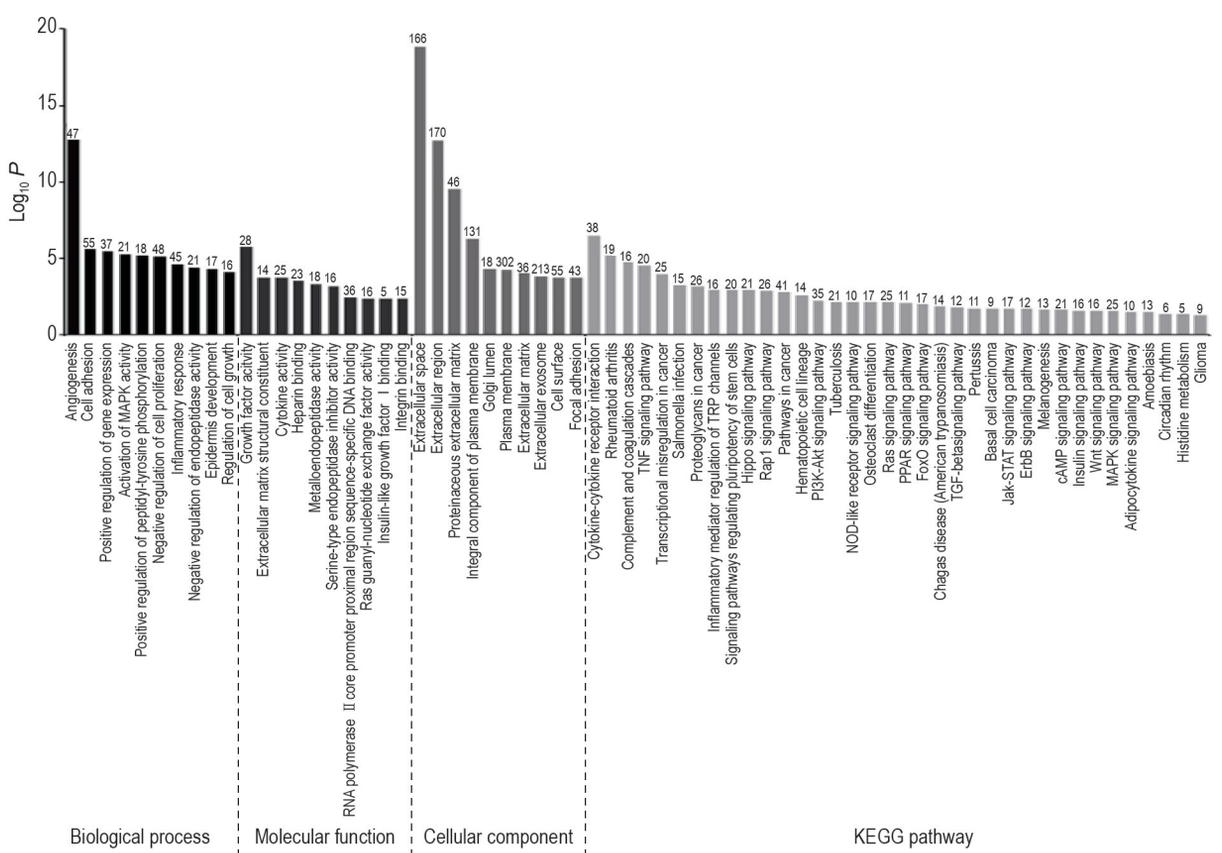

Fig.5 Gene Ontology (GO) and KEGG pathways of differentially expressed genes in THBEc1-Δ*FOXA1*-c34 cells. GO and KEGG pathway were gathered via DAVID database. Top 10 items of each GO term, and all KEGG pathways are shown in the graph. The number at the top of the entry referred to enriched genes.

bisphosphate 3-kinase/protein kinase B, PI3K/Akt)通路,叉头框转录因子O(forkhead box O, FoxO)通路、TGF-β通路和MAPK通路等(图5)。

PPI网络分析发现,349个差异表达基因所编码的蛋白质彼此间存在相互作用并形成复杂的网络(图6A)。进一步分析发现,在此PPI网络中,存在分别以CCL3,GCNT3,MMP3和FZD8作为种子节点的4个核心功能模块(图6B)。这些核心功能模块主要参与免疫应答和炎症反应、O-聚糖加工、胶原分解代谢过程、以及典型WNT通路等。

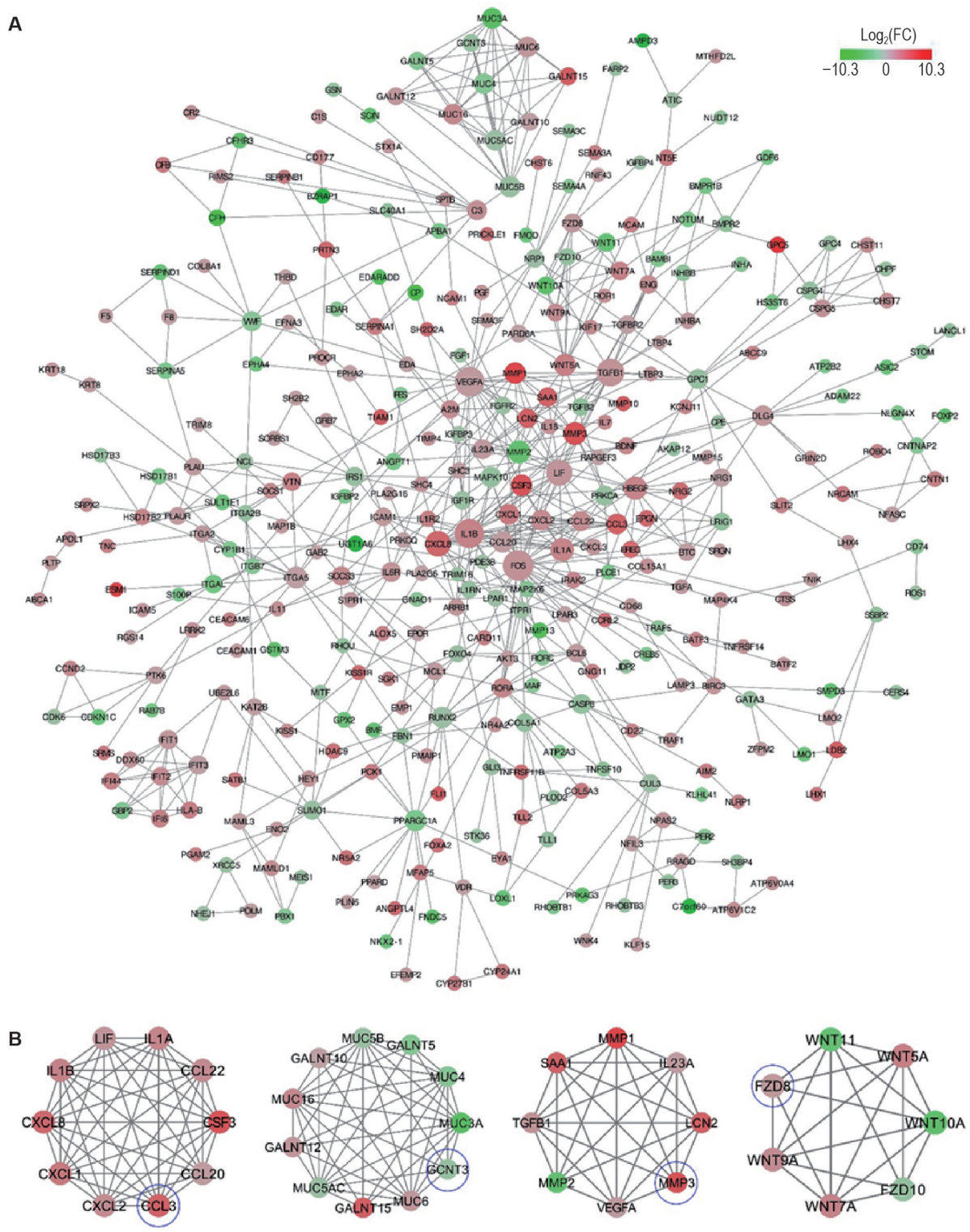

Fig.6 Protein-protein interaction network of proteins encoded by differentially expressed genes. A: the interaction network between proteins encoded by 349 differentially expressed genes created using STRING 11.5 tool, and visualized by Cytoscape 3.8.2 software. B: the top 4 core function modules created via MCODE plug in Cytoscape 3.8.2. The protein in the blue circle box was the seed node.

3 讨论

本研究发现，模型细胞间共1332个基因差异表达，涉及多项GO功能和多条信号通路，包括血管生成、黏附、细胞增殖、炎症反应、基因表达调控、细胞因子-细胞因子受体相互作用、蛋白聚糖、MAPK激活、代谢、免疫应答和细胞外基质分解等多种与肿瘤的发生和发展相关的生物学事件。提示FOXA1可能通过参与调节以上生物学过程影响肿瘤的发生和发展。

TNF通路与细胞增殖、迁移、侵袭和血管生成密切相关[21]。本研究发现，*FOXA1*敲除后，参与TNF通路及与其相关的MAPK通路的多个基因表达发生改变，如*TRAF5*，*MAP2K6*，*MAPK14*，*MAPK10*，*CREB5*和*CASP8*等均表达下调。TRAF5是肿瘤坏死因子相关受体家族成员，可促进肿瘤细胞增殖、迁移和侵袭等[22]。TNF通路可以通过影响MAPK通路发挥作用[23]。MAPK通路是对氧化应激、细胞因子等外界刺激产生反应的关键通路。在多种肿瘤中，MAPK通路被激活，从而促进肿瘤细胞增殖和迁移[24-25]。如有研究发现，Kin17作为一种DNA和RNA结合蛋白，可通过激活P38 MAPK信号通路促进甲状腺癌细胞增殖[26]。LncRNA TUC338通过激活MAPK通路促进肺癌的侵袭潜能[27]。MAPK通路包括ERK，JNK和P38 MAPK 3条经典通路。敲除*FOXA1*后，MAPK信号通路相关基因表达明显改变。ERK通路中Ⅰ型跨膜AMPA受体调节蛋白编码基因*CACNG4*、受体酪氨酸激酶编码基因*IGF1R*和*FGFR2*、蛋白质丝氨酸/苏氨酸激酶编码基因*PRKCA*表达均下调，*DUSP4*和*DUSP5*表达均上调，DUSP4和DUSP5可负调控ERK/JNK。JNK和P38 MAPK信号通路中相关蛋白编码基因*TGFB2*，*MAPK10*，*MAPK14*，*MAP2K6*和*HSPB1*表达均下调。上述TNF和MAPK信号通路多个基因表达失调，提示*FOXA1*敲除可能通过直接或间接干扰TNF和MAPK通路导致THBEc1细胞增殖和迁移能力降低。

在差异表达基因编码蛋白的相互作用网络分析中，本研究发现了分别以CCL3，GCNT3，MMP3和FZD8为种子节点的4个核心功能模块。这些功能模块主要参与免疫应答和炎症反应、黏蛋白型O-聚糖生物合成、胶原分解代谢过程及典型WNT通路等。

WNT通路是调控上皮-间充质转化（epithelial-to-mesenchymal transition，EMT）的重要通路之一，其异常活化与肿瘤发生发展关系密切。WNT蛋白与膜受体Frizzled蛋白结合是启动WNT通路的重要步骤。以FZD8为种子节点的功能模块包含了5种WNT蛋白（WNT5A，WNT7A，WNT9A，WNT10A，WNT11）和2种Frizzled蛋白（FZD8和FZD10）。WNT10A高表达能促进多种肿瘤的迁移、侵袭和增殖[28-30]。载有FZD10和*FZD10* mRNA的外泌体可体外促进多种肿瘤细胞增殖[31]。用小干扰RNA（small interfering RNA，siRNA）干扰*FZD10*表达可抑制肿瘤细胞生长[32]。*FZD10*的表观遗传沉默可抑制WNT3-FZD10-β联蛋白异常活化，从而抑制肿瘤转移[33]。此外，WNT5A的异常激活可以抑制肝癌和乳腺癌细胞的迁移和侵袭[34-35]。*FOXA1*敲除后*WNT10A*和*FZD10*表达均下调，而*WNT5A*表达上调，提示WNT信号通路扰动可能是FOXA1影响THBEc1细胞迁移的重要机制。

以GCNT3为种子节点的功能模块包含11种蛋白，分别是黏蛋白家族的MUC3A，MUC4，MUC5AC，MUC5B，MUC6和MUC16，葡萄糖氨基转移酶家族的GCNT3，以及催化黏蛋白O型糖基化修饰起始酶的N-乙酰氨基半乳糖转移酶家族的GALNT5，GALNT10，GALNT12和GALNT15。黏蛋白异常表达可通过破坏上皮细胞极性，影响细胞间相互作用，促进EMT。MUC3A，MUC4，MUC5AC和MUC5B在非小细胞肺癌和肺粘液腺癌中高表达，并与不良预后有关[36-38]。GCNT3在非小细胞肺癌中表达上调，抑制GCNT3可降低A549细胞增殖、迁移和侵袭能力[39]。*FOXA1*敲除后，上述4种黏蛋白以及GCNT3编码基因均下调，提示其亦可能是*FOXA1*敲除后细胞增殖和迁移能力降低的原因之一。

综上所述，*FOXA1*敲除后BaP恶性转化细胞THBEc1转录组明显改变，增殖和迁移能力降低。敲除*FOXA1*可能通过直接或间接干扰TNF，MAPK和WNT等通路抑制细胞增殖和迁移。FOXA1可能作为BaP致癌的潜在生物标志物和肺癌的潜在治疗靶点。本研究为后续FOXA1的靶基因探索提供了基础，有助于进一步阐明FOXA1在BaP致癌作用中的机制。

参考文献：

[1] Nimura Y, Yokoyama S, Fujimori M, *et al*. Genotyping of the CYP1A1 and GSTM1 genes in esophageal carcinoma patients with special reference to smoking[J]. *Cancer*, 1997, 80(5): 852-857.

[2] Chen X, Peng H, Xiao J, *et al*. Benzo[a]pyrene enhances the EMT-associated migration of lung adenocarcinoma A549 cells by upregulating Twist1[J]. *Oncol Rep*, 2017, 38(4): 2141-2147.

[3] Zhao P, Fu J, Yao B, *et al*. *In vitro* malignant transformation of human bronchial epithelial cells induced by benzo(a)pyrene[J]. *Toxicol In Vitro*, 2012, 26(2): 362-368.

[4] Jiang Y, Wu Y, Greenlee AR, *et al*. miR-106a-mediated malignant transformation of cells induced by anti-benzo[a]pyrene-trans-7, 8-diol-9, 10-epoxide[J]. *Toxicol Sci*, 2011, 119(1): 50-60.

[5] Zhao Y, Liu H, Li Y, *et al*. The role of miR-506 in transformed 16HBE cells induced by anti-benzo[a] pyrene-trans-7, 8-dihydrodiol-9, 10-epoxide[J]. *Toxicol Lett*, 2011, 205(3): 320-326.

[6] Ke X, He L, Wang R, *et al*. miR-377-3p-mediated EGR1 downregulation promotes B[a]P-induced lung tumorigenesis by WNT/beta-catenin transduction[J/OL]. *Front Oncol*, 2021, 11: 699004 (2021-08-23) [2021-09-05]. https://pubmed. ncbi. nlm. nih. gov / 34497759/. DOI: 10.3389/fonc.2021.699004.

[7] Yang Q, Zhang S, Liu H, *et al*. Oncogenic role of long noncoding RNA AF118081 in anti-benzo[a]pyrene-trans-7,8-dihydrodiol-9,10-epoxide-transformed 16HBE cells[J]. *Toxicol Lett*, 2014, 229(3): 430-439.

[8] Hu G, Yang T, Zheng J, *et al*. Functional role and mechanism of lncRNA LOC728228 in malignant 16HBE cells transformed by anti-benzopyrene-trans-7, 8-dihydrodiol-9, 10-epoxide[J]. *Mol Carcinog*, 2015, 54(1): E192-E204.

[9] Gao L, Mai A, Li X, *et al*. LncRNA-DQ786227-mediated cell malignant transformation induced by benzo [a]pyrene[J]. *Toxicol Lett*, 2013, 223(2): 205-210.

[10] Xiao Z, Yang Z, Xu M, *et al*. The Circ_CARM1 controls cell migration by regulating CTNNBIP1 in anti-benzo [a]pyrene-trans-7, 8-dihydrodiol-9, 10-epoxide-transformed 16HBE cells[J]. *Toxicol Lett*, 2021, 348: 40-49.

[11] Magnani L, Eeckhoute J, Lupien M. Pioneer factors: directing transcriptional regulators within the chromatin environment[J]. *Trends Genet*, 2011, 27(11): 465-474.

[12] Carroll JS, Liu XS, Brodsky AS, *et al*. Chromosome-wide mapping of estrogen receptor binding reveals long-range regulation requiring the forkhead protein FoxA1[J]. *Cell*, 2005, 122(1): 33-43.

[13] Lee CS, Friedman JR, Fulmer JT, *et al*. The initiation of liver development is dependent on Foxa transcription factors[J]. *Nature*, 2005, 435(7044): 944-947.

[14] Lin L, Miller CT, Contreras JI, *et al*. The hepatocyte nuclear factor 3 alpha gene, HNF3alpha (FOXA1), on chromosome band 14q13 is amplified and overexpressed in esophageal and lung adenocarcinomas[J]. *Cancer Res*, 2002, 62(18): 5273-5279.

[15] DeGraff DJ, Clark PE, Cates JM, *et al*. Loss of the urothelial differentiation marker FOXA1 is associated with high grade, late stage bladder cancer and increased tumor proliferation[J / OL]. *PLoS One*, 2012, 7(5): e36669 (2012-05-10) [2021-09-05]. https://pubmed.ncbi.nlm.nih.gov/22590586/. DOI: 10.1371/journal.pone.0036669.

[16] Davis DG, Siddiqui MT, Oprea-Ilies G, *et al*. GATA-3 and FOXA1 expression is useful to differentiate breast carcinoma from other carcinomas[J]. *Hum Pathol*, 2016, 47(1): 26-31.

[17] Li J, Zhang S, Zhu L, *et al*. Role of transcription factor FOXA1 in non-small cell lung cancer[J]. *Mol Med Rep*, 2018, 17(1): 509-521.

[18] Xu T, Yan S, Jiang L, *et al*. Gene amplification-driven long noncoding RNA SNHG17 regulates cell proliferation and migration in human non-small-cell lung cancer[J]. *Mol Ther Nucleic Acids*, 2019, 17: 405-413.

[19] Guo W, Keener AL, Jing Y, *et al*. FOXA1 modulates EAF2 regulation of AR transcriptional activity, cell proliferation, and migration in prostate cancer cells [J]. *Prostate*, 2015, 75(9): 976-987.

[20] Wang Y, Li L, Hao M, *et al*. Label-free quantitative proteomic analysis identifies the oncogenic role of FOXA1 in BaP-transformed 16HBE cells[J/OL]. *Toxicol Appl Pharmacol*, 2020, 403: 115160 [2021-09-05]. https://doi.org/10.1016/j.taap.2020.115160.

[21] Wu Y, Zhou BP. TNF-alpha/NF-kappaB/Snail pathway in cancer cell migration and invasion[J]. *Br J Cancer*, 2010, 102(4): 639-644.

[22] Sun G, Zheng C, Deng Z, *et al*. TRAF5 promotes the occurrence and development of colon cancer via the activation of PI3K/AKT/NF-κB signaling pathways[J]. *J Biol Regul Homeost Agents*, 2020, 34(4): 1257-1268.

[23] Ren X, Han L, Li Y, *et al*. Isorhamnetin attenuates TNF-α-induced inflammation, proliferation, and migration in human bronchial epithelial cells via MAPK and NF-κB pathways[J]. *Anat Rec (Hoboken)*, 2021, 304(4): 901-913.

[24] Shin MH, Kim J, Lim SA, *et al*. Current insights into combination therapies with MAPK inhibitors and immune checkpoint blockade[J/OL]. *Int J Mol Sci*, 2020, 21 (7): 2531 (2020-04-05) [2021-09-05]. https://pubmed.

ncbi.nlm.nih.gov/32260561/. DOI:10.3390/ijms210-72531.

[25] Martínez-Limón A, Joaquin M, Caballero M, *et al*. The P38 pathway: from biology to cancer therapy[J/OL]. *Int J Mol Sci*, 2020, 21(6): 1913 (2020-03-11) [2021-09-05]. https://pubmed.ncbi.nlm.nih.gov/3216-8915/. DOI: 10.3390/ijms21061913.

[26] Jiang QG, Xiong CF, Lv YX. Kin17 facilitates thyroid cancer cell proliferation, migration, and invasion by activating P38 MAPK signaling pathway[J]. *Mol Cell Biochem*, 2021, 476(2): 727-739.

[27] Zhang YX, Yuan J, Gao ZM, *et al*. LncRNA TUC338 promotes invasion of lung cancer by activating MAPK pathway[J]. *Eur Rev Med Pharmacol Sci*, 2018, 22(2): 443-449.

[28] Long A, Giroux V, Whelan KA, *et al*. WNT10A promotes an invasive and self-renewing phenotype in esophageal squamous cell carcinoma[J]. *Carcinogenesis*, 2015, 36(5): 598-606.

[29] Li P, Liu W, Xu Q, *et al*. Clinical significance and biological role of Wnt10a in ovarian cancer[J]. *Oncol Lett*, 2017, 14(6): 6611-6617.

[30] Dong T, Zhang Z, Zhou W, *et al*. WNT10A/β-catenin pathway in tumorigenesis of papillary thyroid carcinoma[J]. *Oncol Rep*, 2017, 38(2): 1287-1294.

[31] Scavo MP, Depalo N, Rizzi F, *et al*. FZD10 carried by exosomes sustains cancer cell proliferation[J/OL]. *Cells*, 2019, 8(8): 777 (2019-07-25) [2021-09-05]. https://pubmed.ncbi.nlm.nih.gov/31349740/. DOI: 10.3390/cells8080777.

[32] Nagayama S, Fukukawa C, Katagiri T, *et al*. Therapeutic potential of antibodies against FZD 10, a cell-surface protein, for synovial sarcomas[J]. *Oncogene*, 2005, 24(41): 6201-6212.

[33] Gong C, Qu S, Lv XB, *et al*. BRMS1L suppresses breast cancer metastasis by inducing epigenetic silence of FZD10[J/OL]. *Nat Commun*, 2014, 5: 5406 (2014-11-19) [2021-09-05]. https://pubmed.ncbi.nlm.nih.gov/25406648/. DOI: 10.1038/ncomms6406.

[34] Wakizaka K, Kamiyama T, Wakayama K, *et al*. Role of WNT5A in suppressing invasiveness of hepatocellular carcinoma via epithelial-mesenchymal transition[J/OL]. *Oncol Lett*, 2020, 20(5): 268 (2020-09-21) [2021-09-05]. https://pubmed.ncbi.nlm.nih.gov/32989402/. DOI: 10.3892/ol.2020.12131.

[35] Prasad CP, Chaurasiya SK, Guilmain W, *et al*. WNT5A signaling impairs breast cancer cell migration and invasion via mechanisms independent of the epithelial-mesenchymal transition[J/OL]. *J Exp Clin Cancer Res*, 2016, 35(1): 144 (2016-09-13) [2021-09-05]. https://pubmed.ncbi.nlm.nih.gov/27623766/. DOI: 10.1186/s13046-016-0421-0.

[36] Sun Y, Sun X, You C, *et al*. MUC3A promotes non-small cell lung cancer progression via activating the NFκB pathway and attenuates radiosensitivity[J]. *Int J Biol Sci*, 2021, 17(10): 2523-2536.

[37] Kim YK, Shin DH, Kim KB, *et al*. MUC5AC and MUC5B enhance the characterization of mucinous adenocarcinomas of the lung and predict poor prognosis[J]. *Histopathology*, 2015, 67(4): 520-528.

[38] Hollingsworth MA, Swanson BJ. Mucins in cancer: protection and control of the cell surface[J]. *Nat Rev Cancer*, 2004, 4(1): 45-60.

[39] 孙晓燕. GCNT3表达在非小细胞肺癌中的临床意义[D]. 天津: 天津医科大学, 2019.

Effects of forkhead box protein A1 knockout on transcriptome of benzo[a]pyrene-transformed human bronchial epithelial 16HBE cells

MA Xue[1], LI Lu-di[1], WANG Yu[2], XING Yun-kun[1], FU Juan-ling[1], YAO Bi-yun[1], ZHAO Peng[1]

(1. Department of Toxicology, Beijing Key Laboratory of Toxicology Research and Risk Assessment for Food Safety, School of Public Health, Peking University, Beijing 100191, China; 2. National Institute of Environmental Health, Chinese Center for Disease Control and Prevention, Beijing 100021, China)

Abstract: OBJECTIVE To explore the possible mechanism of forkhead box protein A1 (*FOXA1*) in benzo[a]pyrene (BaP)-induced carcinogenesis by determining changes in transcriptomes of BaP-transformed human bronchial epithelial 16HBE cells (THBEc1) after *FOXA1* gene knockout. **METHODS**

FOXA1 knockout THBEc1 cells THBEc1-Δ*FOXA1*-c34 and control cells THBEc1-ctrl were selected as cell models. Western blotting was used to determine FOXA1 protein expression levels. Colony formation assay and Transwell assay were performed to determine the effects of *FOXA1* knockout on THBEc1 cell proliferation and migration, respectively. Transcriptome sequencing technology was used to analyze and compare transcriptomes between THBEc1-Δ*FOXA1*-c34 and THBEc1-ctrl cells. Real-time quantitative PCR (RT-qPCR) was employed to confirm the transcriptome sequencing findings. The biological information, including Gene Ontology (GO) and KEGG pathway, was retrieved from the DAVID database. STRING 11.5 database and Cytoscape 3.8.2 were used to construct the interaction network of the proteins encoded by differentially expressed genes. **RESULTS** THBEc1-Δ*FOXA1*-c34 cells did not express full-length FOXA1 protein, and their proliferation and migration potential was lower than that of THBEc1-ctrl. A total of 1332 genes were identified as differentially expressed genes (fold change>2 or <0.5, false discovery rate<0.05) via transcriptome sequencing analysis between THBEc1-Δ*FOXA1*-c34 cells and THBEc1-ctrl cells, among which 691 genes were up-regulated and 641 genes were down-regulated in THBEc1-Δ*FOXA1*-c34 cells. The expression differences between 47 genes determined by RT-qPCR were consistent with those of transcriptome sequencing. Differentially expressed genes were involved in many biological processes, including angiogenesis, cell proliferation, migration, adhesion, inflammatory response, immune response, signal transduction〔involving tumor necrosis factor (TNF), mitogen-activated protein kinase (MAPK), phosphatidylinositol-4, 5-bisphosphate 3-kinase/protein kinase B and TGF-β pathways〕and metabolism. In the interaction network formed by the proteins encoded by 349 differentially expressed genes, 4 core functional modules with CCL3, GCNT3, MMP3 and FZD8 as seed nodes, respectively, were found. The core functional modules mainly participated in immune response and inflammatory response, O-glycan processing, collagen catabolic process and canonical WNT pathway. **CONCLUSION** *FOXA1* knockout can lead to significant changes in transcriptomes of BaP-transformed cell THBEc1, and a significant decrease in the proliferation and migration potential. *FOXA1* knockout might directly or indirectly affect TNF, MAPK and WNT pathways, thereby inhibiting cell proliferation and migration. FOXA1 might act as a potential biomarker of BaP-induced carcinogenesis and a potential therapeutic target for lung cancer.

Key words: benzo[a] pyrene; forkhead box protein A1; THBEc1 cells

Foundation item: National Natural Science Foundation of China (81370079); National Natural Science Foundation of China (81001253); and Beijing Natural Science Foundation (7132122)

Corresponding author: ZHAO Peng, E-mail: zhaopeng@bjmu.edu.cn

（收稿日期：2021-09-08 接受日期：2021-11-23）

（本文编辑：魏 霞）